Journal of Molecular Liquids 333 (2021) 116000

Contents lists available at ScienceDirect

Journal of Molecular Liquids

journal homepage: www.elsevier.com/locate/molliq

# An insight into cyclocurcumin cis–trans isomerization: Kinetics in solution and in the presence of silver nanoparticles

Guido Angelini [a], Axel Gansmüller [b], Jérémy Pécourneau [c], Carla Gasbarri [a,*]

[a] Department of Pharmacy, University "G. d'Annunzio" of Chieti-Pescara, via dei Vestini, 66100 Chieti, Italy
[b] CRM2 UMR CNRS 7036, Université de Lorraine, 54506 Vandœuvre-lès-Nancy, France
[c] L2CM UMR CNRS 7053, Université de Lorraine, 54506 Vandœuvre-lès-Nancy, France

ARTICLE INFO

*Article history:*
Received 15 February 2021
Revised 22 March 2021
Accepted 26 March 2021
Available online 6 April 2021

*Keywords:*
Cyclocurcumin
Kinetic rate constants
Polarizability
Silver nanoparticles
Solvatochromism
Catalán solvent scale

ABSTRACT

Cyclocurcumin (CyCUR) is a non-diarylheptanoid curcuminoid characterized by an α,β-unsaturated dihydropyranone moiety generally existing as trans isomer in the ground state but able to convert into the cis form by photoisomerization. Herein the kinetics of thermal cis–trans isomerization of cyclocurcumin was spectroscopically determined in ethanol, pure water and silver nanoparticles (AgNPs) aqueous solution. Energetic parameters were calculated by Arrhenius and Eyring plots in the temperature range 294–314 K. The presence of AgNPs increases the rate of the reaction, according to the polarizability of the environment. The solvatochromism of cyclocurcumin was also studied by using the Catalán empirical solvent parameters scale in a series of organic solvents. The bathochromic shift of CyCUR suggests that polarizability of the medium plays the major role in the investigated conditions.



## 1. Introduction

Generally, the bioactive behavior of curcuminoids, natural polyphenols isolated from *Curcuma Longa* L., is attributed to curcumin, the major component in turmeric followed by demethoxycurcumin, bisdemethoxycurcumin and cyclocurcumin [1–3]. In some cases, synergic effects in using their mixtures were observed [4,5]. Except for cyclocurcumin, curcuminoids exhibit diketo/keto-enol tautomerism in solution due to the presence of the β-diketone moiety and most of their properties seem to be dependent on the enol concentration [6,7].

Interestingly, antioxidant, anti-vasoconstrictive, immune-modulating and neuroprotective effects of cyclocurcumin were recently reported [8–11]. Cyclocurcumin is a non-diarylheptanoid curcuminoid characterized by an α,β-unsaturated dihydropyranone moiety which excludes diketo/keto-enol tautomerism but allows trans–cis photoisomerization by rotation around the ethylenic double bound (Scheme 1). The molecule exists entirely as trans isomer in both nature and solution and can be converted to cis form by exposition to light. Interestingly, it was observed that the physicochemical properties of the environment, such as polarity and viscosity, may affect the fluorescence quantum yield of the isomers [12,13].

Generally, isomerization reactions are involved in a large variety of applications, including light-sensitive devices, due to the spectral differences between the isomers [14–18]. Despite cyclocurcumin exhibits a photophysical behavior, the trans to cis photoisomerization is still rarely investigated, while the thermal cis to trans conversion was very marginally reported. The aim of our work was to kinetically study the thermal cis–trans isomerization of cyclocurcumin in three eco-friendly environments, as ethanol, pure water and AgNPs aqueous solution. The activation energy ($E_a$), the frequency factor (A), the activation enthalpy ($\Delta H^{\neq}$) and the activation entropy ($\Delta S^{\neq}$) were calculated for each environment in the temperature range 294–314 K. Additionally, the photostationary state of CyCUR was observed for the first time by using in situ photo-NMR spectroscopy.

The solvatochromism of CyCUR was also studied in a series of organic solvents at 298 K and the contribute of each solvent parameter, as polarizability (SP), dipolarity (SdP), acidity (SA) and basicity (SB) was extrapolated by using the Catalán multiparametric empirical solvent parameters scale. To the best of our knowledge the kinetics of the cis–trans isomerization and solvatochromism of cyclocurcumin in the investigated conditions were unprecedented.

* Corresponding author.
*E-mail address:* carla.gasbarri@unich.it (C. Gasbarri).

https://doi.org/10.1016/j.molliq.2021.116000
0167-7322/

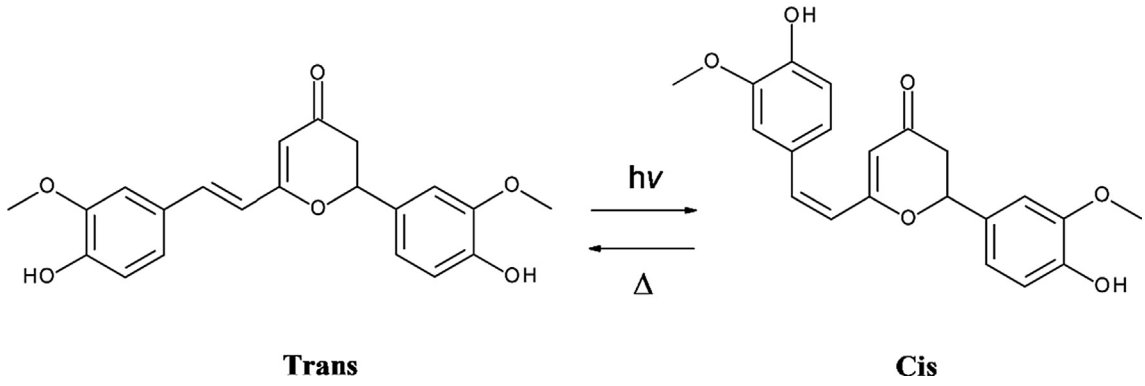


**Scheme 1.** Representation of the trans–cis and cis–trans isomerization of cyclocurcumin.

## 2. Experimental

### 2.1. Materials

Cyclocurcumin powder (purity 99%) was purchased from MuseChem. All solvents (ethanol, methanol, tetrahydrofuran, acetonitrile, chloroform, toluene, cyclohexane, 1,4-dioxane, isooctane, acetic acid, acetone, 1-octanol, 1-pentanol, ethyl acetate, *N*,*N*-dimethylformamide, 2-propanol, dimethyl sulfoxide, 99% solvent spectroscopy grade) were purchased from Sigma-Aldrich. Silver nanoparticles (0.02 mg/mL) was purchased from AlfaAesar. All reagents were used without further purification.

### 2.2. Sample preparation

Milli-Q water was used for the preparation of the AgNPs solutions (2 ppm; pH 5.5). Stock ethanolic solution of cyclocurcumin was prepared at a concentration of $3 \times 10^{-3}$ M and kept in the dark at room temperature. Then, an aliquote of the solution was transferred to 1 cm light path quartz thermostated cuvette containing 2 mL of the solvent to obtain a CyCUR final concentration of $1.0 \times 10^{-5}$ M.

### 2.3. Kinetic measurements

The sample was irradiated for 10 min in the temperature range 294–314 K by using a Hg arc lamp (200 W) equipped with a band-pass interference filter centered at 365.0 + 2/−0 nm wavelength and 10.0 +2/−2 nm bandwidth in order to induce the photoisomerization of cyclocurcumin. The UV–vis spectra were recorded at the investigated temperature by using a spectrophotometer Jasco V570. The decreasing of the high-intensity absorption band and the simultaneous increasing of the peak at lower wavelength were used as evidence for the trans–cis conversion of the sample. Similar spectra changes were obtained by irradiation with a filter centered at 254 nm and 436 nm (Supporting Material). The thermal cis–trans isomerization was spectrophotometrically followed by recording the absorption increasing as a function of time in the dark under stirring. The kinetics of the reaction follows a first-order profile and the corresponding first-order rate constants, ($k_{obs}$) in the temperature range 294–314 K were determined according to Eq. (1):

$$\ln(A_{inf} - A_t) = k_{obs}t \quad (1)$$

where $A_{inf}$ and $A_t$ are the absorbance of the sample before irradiation and the time-dependent absorbance, respectively.

The activation energy ($E_a$) and the pre-exponential factor (A) were calculated from the Arrhenius plot according to Eq. (2):

$$\ln k_{obs} = \ln A - E_a/RT \quad (2)$$

where $R$ is the universal gas constant and T is the absolute temperature.

The activation enthalpy ($\Delta H^{\neq}$) and the activation entropy ($\Delta S^{\neq}$) were obtained by the

Eyring plot according to Eq. (3):

$$\ln(k_{obs}/T) = -\Delta H^{\neq}/RT + \ln(K_B/h) + \Delta S^{\neq}/R \quad (3)$$

where $K_B$ and $h$ are the Bolzmann and Planck constants, respectively.

### 2.4. HPLC measurements

HPLC analysis were performed on ThermoFischer instrument equipped with TSP 2000 pump, UV6000LP DAD detector. A chiral column *R*,*R*-DACH-DBN, 250 × 4.6 mm, 5 μm, was used at 30 °C with methanol 70% as eluent, 0.7 mL/min. The sample (20 μL) was injected before and after irradiation at 365 nm. Toluene was added as internal standard.

### 2.5. Solvatochromic measurements

The solvent-dependent wavenumbers of the maximum adsorption band ($\nu_{max}$) were obtained from the spectrophotometrically determined $\lambda_{max}$ at 298 K in a series of organic solvents (ethanol, methanol, tetrahydrofuran, acetonitrile, chloroform, toluene, cyclohexane, 1,4-dioxane, isooctane, acetic acid, acetone, 1-octanol, 1-pentanol, ethyl acetate, *N*, *N*-dimethylformamide, 2-propanol, dimethyl sulfoxide) and water. The Catalán empirical parameters, as solvent polarizability (SP), solvent dipolarity (SdP), solvent acidity (SA) and solvent basicity (SB) were correlated to the $\nu_{max}$ by multiple linear regression analysis [19], according to Eq. (4):

$$\nu_{max} = \nu_0 + C_1(SP) + C_2(SdP) + C_3(SA) + C_4(SB) \quad (4)$$

where $\nu_0$ corresponds to the extrapolated value of $\nu_{max}$ in gaseous state, while $C_1$, $C_2$, $C_3$ and $C_4$ are solvent-independent coefficients related to the single contributions of the respective solvatochromic parameters [20,21].

### 2.6. NMR spetroscopy measurements

NMR analysis was performed on a Bruker Avance III HD 300 MHz spectrometer equipped with a 5 mm BBO probehead. All NMR data were processed using TopSpin (Bruker) software.

One dimensional $^1$H NMR measurements were acquired with 65k points over a 6009 Hz frequency window centered at 6.17 ppm. 16 scans were accumulated with an interscan delay of 2 s with 4 preceding dummy scans. Two dimensional $^1$H-COSY experiments were acquired with 8 k points over a 3606 Hz

frequency window centered at 5 ppm in the direct dimension and 512 points over 3094 Hz centered at 5 ppm in the indirect dimension. 8 scans were accumulated with an interscan delay of 2 s with 4 preceding dummy scans. In situ sample irradiation was performed by directly coupling a 375 nm LED (Thorlabs, M375L4) with a 400 μm multimode optical fiber (Thorlabs, FG400AEA, 0.22 NA). At the tip of the fiber, the jacket was removed and the fiber was inserted into a coaxial insert tube filled with $D_20$. This coaxial tube was then inserted in the 5 mm NMR tube containing the cyclocurcumin sample dissolved in DMSO at the concentration of $5.4 \times 10^{-3}$ M. This setup (Fig. I in Supplementary Material) was inpired from the work from Feldmeier et al. [22], but the length of the fiber was adjusted to shine light from above the coil measurement area onto the sample solution. The role of the coaxial insert was to center the fiber inside the NMR tube and allow a more homogeneous "radial type" irradiation with a light path length of about 0.1 cm since the insert in the center of the NMR tube is filled with transparent $D_2O$. The light intensity of 1 mW, emitted from the fiber tip, was measured with a powermeter by immersing the tip in an integrating sphere (thorlabs).

## 3. Results and discussion

The UV–vis spectra of cyclocurcumin in ethanol were recorded before and after irradiation at 365 nm for 10 min in the temperature range 294–314 K by using a Hg arc lamp (200 W) as described in the Experimental Section. Before irradiation the spectrum shows a maximun absorption band at 370 nm according to the data previously reported [12] and weak intensity peaks at 233, 260 and 286 nm.

The spectral changes induced by irradiation consist in the decreasing of the absorption band at 370 nm from 0.88 to 0.64 and the simultaneous increasing of the peak at 286 nm from 0.20 to 0.23 in the investigated conditions. Moreover, the ratio between the absorbance at 370 and 286 nm is 4.60 before irradiation and 2.80 after irradiation: this decreasing is most reasonably due to the conversion of a part of the trans isomer into the cis form in agreement with the spectral behavior of a natural photoswitch as resveratrol [23]. In Fig. 1 the UV–vis spectra of CyCUR at 298 K before and after irradiation at 365 nm was reported as an example.

The presence of the cis isomer after irradiation was tested by HPLC analysis. The peaks shape of an on-column interconversion is usually observed as a profile between the two resolved peaks that does not reach the baseline. In most cases the cis–trans isomerism is significantly fast and does not enable the separation of isomers [24,25]. The dynamic chromatogram obtained after the irradiation of cyclocurcumin in ethanol (Fig. 2) could be attributed to two resolvable stereoisomers interconverting on the separation time scale.

Deeper insights on the photoisomerization process are provided by in situ photo-NMR measurements where the products of the photoisomerization and thermal back reaction can be monitored directly during the irradiation and temperature treatments. NMR measurements on the *cis*-CyCUR photoisomer have not been reported before and our approach allows the measurement and assignment of the photoproduct along with the observation of curcumin as a thermal degradation product. Clear evidence for the photoisomerization is the reduction of the homonuclear $^3$J ethylenic $^1$H coupling from 16 Hz (trans isomer) to 12.8 Hz (cis isomer). Fig. 3 shows that upon irradiation, the signals from *trans*-CyCUR (3.812/3.808 ppm) are reduced in favor of the appearance of the signals from *cis*-CyCUR (3.678/3.773 ppm). After about 12 h irradiation a photostationary state is reached, resulting in the production of 44% cis isomer (Fig. 3b). These signals subsequently disappear when irradiation is turned off and the sample is heated up to 353 K for a few hours (Fig. 3c). The return to the same photostationary state as before heating is then verified for a second irradiation step (Fig. 3d). As can be observed, an additional signal is present on the spectra; this signal resonating at 3.845 ppm corresponds to the methoxy $^1$H signal from curcumin. From the comparison between the spectra, it is clear that curcumin results from irreversible thermal degradation of CyCUR since the amount increases to 14% after the heating process (Fig. 3c) and no further increase is observed despite a new irradiation step. The full $^1$H NMR spectra with peak assignment, along with the spectral signatures for the individual species can be found in the Supporting Material (Fig. J and K).

From the results of these different characterizations, it is possible to assume that irradiation around 370 nm mainly results in trans to cis photoisomerization and that significant thermal degradation towards curcumin occurs after high temperature treatment.

Kinetic rate constants can be spectroscopically measured for different reaction [26,27]. The kinetics of the cis–trans isomerization of CyCUR was determined in ethanol in the temperature range 294–314 K. The first-order kinetic rate constants ($k_{obs}$) were spectroscopically obtained by monitoring the absorption increasing at the maximum wavelength in the dark as a function of time. The first-order kinetic profile obtained at 314 K was shown in Fig. 4 as an example.

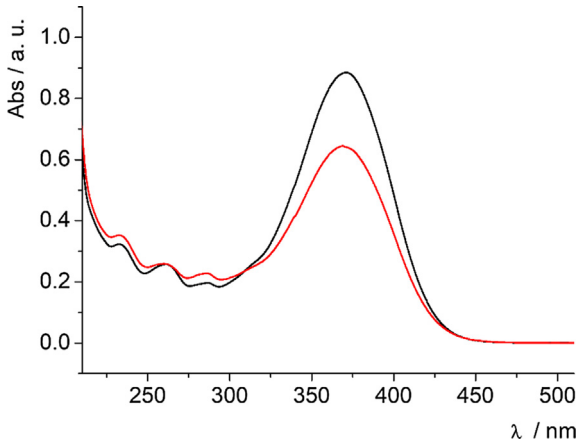


**Fig. 1.** UV–vis spectra of $3 \times 10^{-5}$ M CyCUR in ethanol before (black line) and after irradiation (red line) at 365 nm.

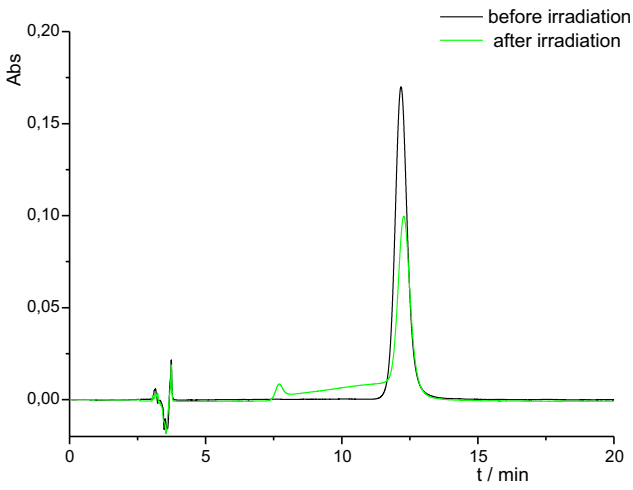


**Fig. 2.** Chromatograms of CyCUR in ethanol injected before (black line) and after irradiation (green line) at 365 nm.

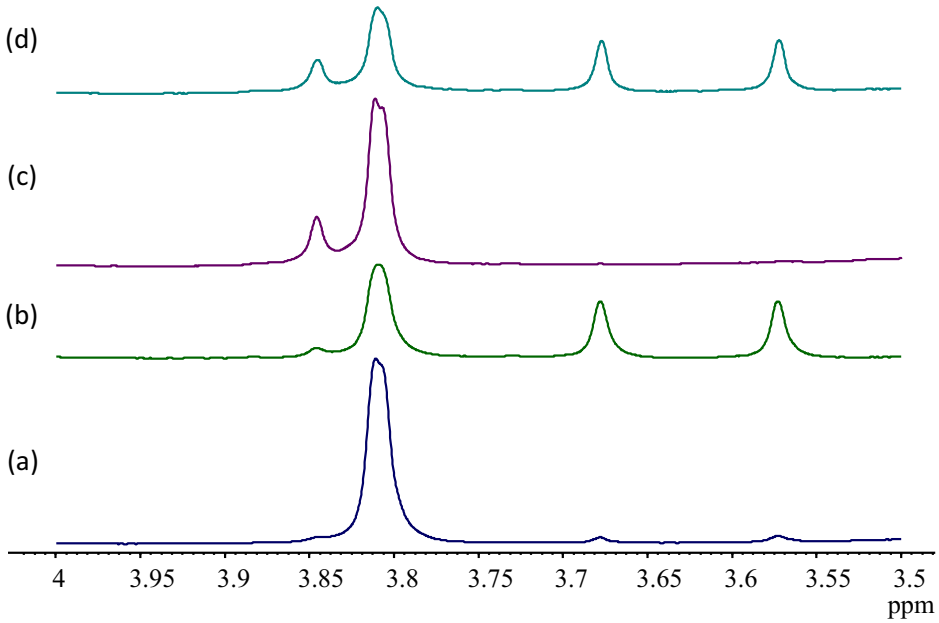


**Fig. 3.** Evolution of the $^{1}$H NMR spectra of $5.4 \times 10^{-3}$ M cyclocurcumin in DMSO, upon successive in-situ irradiation (375 nm) and heating (353 K) steps. (a) Spectrum before irradiation at 310 K. (b) Spectrum after 18 h irradiation at 310 K. (c) Spectrum acquired at 310 K after heating to 353 K for 22 h. (d) Spectrum after re-irradiating for 18 h at 310 K. For clarity, only the MeOH region (4–3.5 ppm) is displayed. Full spectra are displayed in Supplementary Material (Figure J).

The $k_{obs}$ were determined in ethanol, pure water and AgNPs in the investigated temperature range as reported in Table 1.

Generally, temperature tends to enhance the isomerization rate in solution [28] and a similar trend can be observed in the case of cyclocurcumin in the investigated conditions. The cis–trans conversion of CyCUR occurs faster in pure water than in ethanol at each temperature. Interestingly, further increasing in the $k_{obs}$ values were observed in the presence of AgNPs confirming their catalytic activity [29–31]. The Arrhenius and the Eyring plots lead to linear relationships (Supporting Material) and the energetic parameters calculated from Eq. (2) and Eq. (3) are reported in Table 2.

Since both $E_a$ and $\Delta H^{\#}$ depend on the solute–solvent interactions involved in the initial state of the thermal cis–trans isomerization that consists in the solvation of the cis isomer [32] the lower $E_a$ and $\Delta H^{\#}$ suggest a better solvation of CyCUR in ethanol in comparison to pure water and AgNPs aqueous solution. Moreover, since largest $\Delta S^{\#}$ implies largest A value and reflects faster isomerization rates [18,33] the energetic parameters trend is in agreement with the kinetic data by which the cis–trans isomerization of CyCUR in AgNPs aqueous solution is improved in comparison to ethanol and pure water. Recently [34], it was observed that the rate of cis–trans isomerization of azobenzene derivatives increases when the dipole moment of the molecule in the transition state is higher than the dipole moment of the cis isomer: the $k_{obs}$ measured in the presence of AgNPs suggest that the negatively charged nanoparticles might promote the isomerization of the dipolar cis form of CyCUR as previously observed in the case of 4-methoxyazobenzene [35]. The solvent effect in term of polarizability and dipolarity was determined by using the Catalán empirical solvent scale. The solvatochromism of cyclocurcumin was described from the wavenumber maximum absorption value ($\nu_{max}$) in the series of organic solvents (Supporting Material). The normalized UV–vis spectra of CyCUR in isooctane, 1,4-dioxane, *N*,

**Table 1**
Kinetic rate constant values ($k_{obs}$) of the CyCUR cis–trans isomerization in the investigated media.

| T/K | Ethanol $k_{obs}/10^{-3}$ s$^{-1}$ | Pure water $k_{obs}/10^{-3}$ s$^{-1}$ | AgNPs solution $k_{obs}/10^{-3}$ s$^{-1}$ |
|---|---|---|---|
| 294 (±0.1) | 1.30 (±0.01) | 1.65 (±0.01) | 1.93 (±0.02) |
| 298 (±0.1) | 1.83 (±0.01) | 2.31 (±0.02) | 2.96 (±0.01) |
| 302 (±0.1) | 2.64 (±0.02) | 3.73 (±0.02) | 4.54 (±0.01) |
| 306 (±0.1) | 3.59 (±0.01) | 5.51 (±0.01) | 6.93 (±0.02) |
| 310 (±0.1) | 5.01 (±0.02) | 8.00 (±0.01) | 10.9 (±0.03) |
| 314 (±0.1) | 6.77 (±0.01) | 11.2 (±0.01) | 16.0 (±0.03) |

**Table 2**
Activation energy ($E_a$), pre-exponential factor (A), activation enthalpy ($\Delta H^{\#}$) and activation entropy ($\Delta S^{\#}$) for the cis–trans isomerization of CyCUR in the investigated conditions.

| | Ethanol | Pure water | AgNPs solution |
|---|---|---|---|
| $E_a$/kJ mol$^{-1}$ | 63.8 | 75.2 | 81.9 |
| A/s$^{-1}$ | $2.50 \times 10^{8}$ | $3.55 \times 10^{10}$ | $6.56 \times 10^{11}$ |
| $\Delta H^{\#}$/kJ mol$^{-1}$ | 61.1 | 72.7 | 79.3 |
| $\Delta S^{\#}$/JK$^{-1}$mol$^{-1}$ | −92.2 | −51.1 | −27.2 |

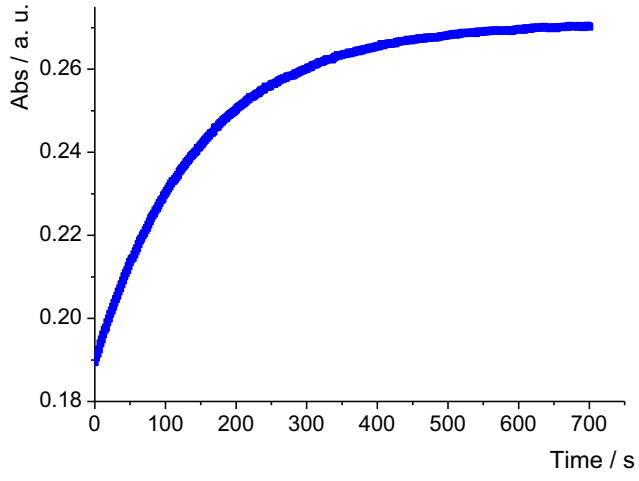


**Fig. 4.** Kinetic profile of CyCUR cis–trans isomerization in ethanol at 314 K.

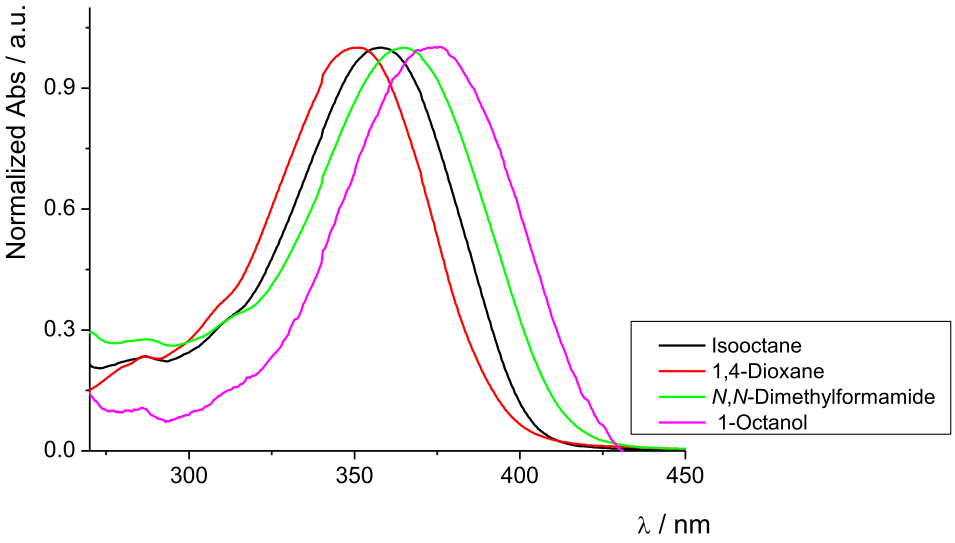


**Fig. 5.** Normalized UV–vis spectra of CyCUR in different solvents at 298 K.

*N*-dimethylformamide and 1-octanol are shown in Fig. 5 as an example.

The solvent parameters as polarizability (SP), solvent dipolarity (SdP), solvent acidity (SA) and solvent basicity (SB) were correlated to the measured $\nu_{max}$ in a multiparametric regression analysis according to Eq. (4). The solvent-independent correlation coefficients $C_1$, $C_2$, $C_3$ and $C_4$, the correlation coefficient R, the number of solvents *n*, the standard deviation SD and the significance *f* for the solvatochromism of CyCUR are reported in Eq. (5):

$$\nu_{max}(10^3 cm^{-1}) = 30.839 - 3.390SP - 0.116SdP - 1.411SA - 1.330SB \quad (5)$$

$(R = 0.9332; n = 18; SD = 0.256; f < 0.0001)$.

The negative algebraic sign of all the correlation coefficients indicate a positive solvatochromism for CyCUR in the investigated series of solvents [36]. Moreover, the highest absolute values of $C_1$ over $C_2$ suggests that polarizability plays the major role in the solute–solvent interactions in comparison to dipolarity [37], while $C_3$ and $C_4$ seem to indicate that also acid-base interactions occur. The quantification of the solvent parameters as percentage contribution are 54% for the polarizability, 2% for dipolarity, 23 and 21% for the solvent acidity and basicity, respectively.

## 4. Conclusion

Irradiation with UV (365 nm) or visible light (436 nm) can trigger the trans–cis photoisomerization of cyclocurcumin in solution. The $^1$H NMR spectrum of CyCUR at the photostationary state and HPLC analysis demonstrate the presence of cis isomer. The cis–trans thermal kinetic rate constants were determined in ethanol, pure water and AgNPs aqueous solution. In particular higher values were measured in the presence of silver nanoparticles in the temperature range 294–314 K. The spectral behavior of CyCUR in a series of organic solvent at 298 K indicates that polarizability represents the dominant parameter over dipolarity, acidity and basicity in the investigated conditions, according to the Catalán empirical multiparametric approach.

The results reported herein are unprecedented and allow the CyCUR to be included in the class of photoswitches and solvatochromic molecules extending the application range to the development of photoreactive-based materials and to the characterization of solvents, respectively. Moreover, the interaction between CyCUR and AgNPs may favour the design of bioactive supramolecular systems as recently demonstrated for curcumin-AgNPs association [38,39].

## CRediT authorship contribution statement

**Guido Angelini:** Methodology, Formal analysis, Investigation, Data curation, Resources, Writing - review & editing. **Axel Gansmüller:** Investigation for NMR analysis and NMR data presentation. **Jérémy Pécourneau:** Investigation for NMR analysis. **Carla Gasbarri:** Conceptualization, Methodology, Investigation, Visualization, Writing - original draft, Writing - review & editing.

## Declaration of Competing Interest

The authors declare that they have no known competing financial interests or personal relationships that could have appeared to influence the work reported in this paper.

## Acknowledgements

This work was supported by Italian Ministry of Education MIUR (60% Grant 2020) and University "G. d'Annunzio" of Chieti-Pescara. A. Gansmüller and J. Pécourneau gratefully acknowledge the European Regional Development Funds (Programme opérationnel FEDER-FSE Lorraine et Massif des Vosges 2014-2020/"Fire Light" project: "Photo-bio-active molecules and nanoparticles") for their financial support.

## Appendix A. Supplementary material

Supplementary data to this article can be found online at https://doi.org/10.1016/j.molliq.2021.116000.

## References

[1] B.B. Aggarwal, K.B. Harikumar, Potential therapeutic effects of curcumin, the anti-inflammatory agent against neurodegenerative, cardiovascular, pulmonary, metabolic, autoimmune and neoplastic diseases, Int. J. Biochem. Cell. Biol. 41 (1) (2009) 40–59.
[2] V.P. Menon, A.R. Sudheer, Antioxidant and anti-inflammatory properties of curcumin, Adv. Med. Biol. 595 (2007) 105–125.

[3] S.C. Gupta, S. Patchva, W. Koh, B.B. Aggarwal, Discovery of Curcumin, a Component of the Golden Spice, and Its Miraculous Biological Activities, Clin. Exp. Pharmacol. Physiol. 39 (3) (2012) 283–299.
[4] F. Kiuchi, Y. Goto, N. Sugimoto, N. Akao, K. Kondo, Y. Tsuda, Nematocidal activity of turmeric: synergic action of curcuminoids, Chem. Pharm. Bull. 41 (1993) 1640–1643.
[5] T. Ahmed, A.H. Gilani, Therapeutic potential of turmeric in Alzheimer's disease: curcumin or curcuminoids?, Phytoter. Res. 28 (2014) 517–525.
[6] D. Yanagisawa, N. Shirai, T. Amatsubo, H. Taguchi, K. Hirao, M. Urushitani, S. Morikawa, T. Inubushi, M. Kato, F. Kato, K. Morino, H. Kimura, I. Nakano, C. Yoshida, T. Okada, M. Sano, Y. Wada, K.N. Wada, A. Yamamoto, I. Tooyama, Relationship between the tautomeric structures of curcumin derivatives and their Abeta-binding activities in the context of therapies for Alzheimer's disease, Biomaterials 31 (2010) 4179–4185.
[7] K.I. Priyadarsini, Photophysics, photochemistry and photobiology of curcumin: Studies from organic solutions, bio-mimetics and living cells, J. Photochem. Photobiol. C: Photochem. Rev. 10 (2009) 81–95.
[8] M. Fu, L. Chen, L. Zhang, X. Yu, Q. Yang, Cyclocurcumin, a curcumin derivative, exhibits immune-modulating ability and is a potential compound for the treatment of rheumatoid arthritis as predicted by the MM-PBSA method, Int. J. Mol. Med. 39 (2017) 1164–1172.
[9] Y. Li, M. Toscano, G. Mazzone, N. Russo, Antioxidant properties and free radical scavenging mechanisms of cyclocurcumin, New J. Chem. 42 (2018) 12698–12705.
[10] K. Kim, J.J. Kim, Y. Jung, J.Y. Noh, A.S. Syed, C.Y. Kim, M.Y. Lee, K.M. Lim, O.N. Bae, J.H. Chung, Cyclocurcumin, an antivasoconstrictive constituent of curcuma longa (turmeric), J. Nat. Prod. 80 (2017) 196–200.
[11] R. Randino, M. Grimaldi, M. Persico, A. De Santis, E. Cini, W. Cabri, A. Riva, G. D'Errico, C. Fattorusso, A.M. D'Ursi, M. Rodriquez, Investigating the neuroprotective effects of turmeric extract: structural interactions of β-amyloid peptide with single curcuminoids, Sci. Rep. 6 (2016) 38846.
[12] R. Adhikary, C.A. Barnes, R.L. Trampel, S.J. Wallace, T.W. Kee, J.W. Petrich, Photoinduced trans-to-cis isomerization of cyclocurcumin, J. Phys. Chem. B 115 (2011) 10707–10714.
[13] M. Marazzi, A. Francés-Monerris, M. Mourer, A. Pasc, A. Monari, Trans-to-cis photoisomerization of cyclocurcumin in different environments rationalized by computational photochemistry, Phys. Chem. Chem. Phys. 22 (2020) 4749–4757.
[14] C.L. Sun, C. Wang, R. Boulatov, Applications of photoswitches in the storage of solar energy, ChemPhotoChem 3 (2019) 268–283.
[15] L. Laprell, K. Hüll, P. Stawski, C. Schön, S. Michalakis, M. Biel, M.P. Sumser, D. Trauner, Restoring light sensitivity in blind retinae using a photochromic AMPA receptor agonist, ACS Chem. Neurosci. 7 (2016) 15–20.
[16] K.S. Schanze, T.F. Mattox, D.G. Whitten, Correlation of the rate of thermal cis-trans isomerization of p–nitro–p′–(dialkylamino)azobenzenes with solvent Z value applied to study polarity in aqueous surfactant solutions, J. Am. Chem. Soc. 104 (6) (1982) 1733–1735.
[17] E. Titov, L. Lysyakova, N. Lomadze, A.V. Kabashin, P. Saalfrank, S. Santer, Thermal cis-to-trans isomerization of azobenzene-containing molecules enhanced by gold nanoparticles: an experimental and theoretical study, J. Phys. Chem. C 119 (2015) 17369–17377.
[18] J. Doki'c, M. Gothe, J. Wirth, M.V. Peters, J. Schwarz, S. Hecht, P. Saalfrank, Quantum chemical investigation of thermal cis-to-trans isomerization of azobenzene derivatives: substituent effects, solvent effects, and comparison to experimental data, J. Phys. Chem. A 113 (2009) 6763–6773.
[19] J. Catalán, Toward a generalized treatment of the solvent effect based on four empirical scales: dipolarity (SdP, a new scale), polarizability (SP), acidity (SA), and basicity (SB) of the medium, J. Phys. Chem. B 113 (2009) 5951–5960.
[20] C. Gasbarri, G. Angelini, Polarizability over dipolarity for the spectroscopic behavior of azobenzenes in room-temperature ionic liquids and organic solvents, J. Mol. Liquids 229 (2017) 185–188.
[21] G. Angelini, C. Gasbarri, Solvent scales comparison by using α-nitrocyclohexanone as probe in ionic liquids, organic solvents and $CH_3CN$/$CHCl_3$ mixtures, Tetrahedron 73 (2017) 3036–3039.
[22] C. Feldmeier, H. Bartling, E. Riedle, R.M. Gschwind, LED based NMR illumination device for mechanistic studies on photochemical reactions–versatile and simple, yet surprisingly powerful, J. Magn. Reson. 232 (2013) 39–44.
[23] L. Camont, C.H. Cottart, Y. Rhayem, V. Nivet-Antoine, R. Djelidi, F. Collin, J.L. Beaudeux, D. Bonnefont-Rousselot, Simple spectrophotometric assessment of the trans-/cis-resveratrol ratio in aqueous solutions, Anal Chim Acta 634 (1) (2009) 121–128.
[24] C. Wolf, Stereolabile chiral compounds: analysis by dynamic chromatography and stopped-flow methods, Chem. Soc. Rev. 34 (2005) 595–608.
[25] C. Dugave, L. Demange, Cis−Trans Isomerization of Organic Molecules and Biomolecules: Implications and Applications, Chem. Rev. 103 (2003) 2475–2532.
[26] P. De Maria, A. Fontana, C. Gasbarri, G. Siani, The effects of cationic and zwitterionic micelles on the keto–enol interconversion of 2-phenylacetylfuran and 2-phenylacetylthiophene, Tetrahedron 61 (2005) 7176–7183.
[27] C. Gasbarri, G. Angelini, A. Fontana, P. De Maria, G. Siani, I. Giannicchi, A. Dalla Cort, Kinetics of demetallation of a zinc–salophen complex into liposomes, Biochim. Biophys. Acta (1818, 2012,) 747–752.
[28] T. Asano, T. Okada, S. Shinkai, K. Shigematsu, Y. Kusano, O. Manabe, Temperature and pressure dependences of thermal cis-to-trans isomerization of azobenzenes which evidence an inversion mechanism, J. Am. Chem. Soc. 103 (1981) 5161–5165.
[29] Y. Xia, Z. Tang, Monodisperse inorganic supraparticles: formation mechanism, properties and applications, Chem. Comm. 48 (2012) 6320–6336.
[30] M. Canamares, J. Garcia-Ramos, J. Gomez-Varga, C. Domingo, S. Sanchez-Cortes, Comparative study of the morphology, aggregation, adherence to glass, and surface-enhanced Raman scattering activity of silver nanoparticles prepared by chemical reduction of $Ag^+$ using citrate and hydroxylamine, Langmuir 21 (2005) 8546–8553.
[31] G. Angelini, A. Pasc, C. Gasbarri, Curcumin in silver nanoparticles aqueous solution: Kinetics of keto-enol tautomerism and effects on AgNPs, Colloids and Surfaces A 603 (2020) 125235.
[32] K. Baba, H. Ono, E. Itoh, S. Itoh, K. Noda, T. Usui, K. Ishihara, M. Inamo, H.D. Takagi, T. Asano, Kinetic study of thermal Z to E isomerization reactions of azobenzene and 4-dimethylamino-4'-nitroazobenzene in ionic liquids [1-R-3-methylimidazolium bis(trifluoromethylsulfonyl) imide with R = butyl, pentyl, and hexyl], Chem. Eur. J. 12 (2006) 5328–5333.
[33] G. Angelini, C. Campestre, L. Scotti, C. Gasbarri, Kinetics and Energetics of Thermal Cis-Trans Isomerization of a Resonance-Activated Azobenzene in BMIM-Based Ionic Liquids for $PF_6^-$/$Tf_2N^-$ Comparison, Molecules 22 (2017) 1273.
[34] X.M. Liu, X. Jin, Z.X. Zhang, J. Wang, F.Q. Bai, Theoretical study on the reaction mechanism of the thermal cis–trans isomerization of fluorine-substituted azobenzene derivatives, RSC Adv. 8 (2018) 11580–11588.
[35] G. Angelini, L. Scotti, A. Aceto, C. Gasbarri, Silver nanoparticles as interactive media for the azobenzenes isomerization in aqueous solution: from linear to stretched kinetics, J. Mol. Liquids 284 (2019) 592–598.
[36] A. Schade, K. Schreiter, T. Rïffer, H. Lang, S. Spange, Interactions of enolizable barbiturate dyes, Chem. Eur. J. 22 (2016) 5734–5748.
[37] J. Catalán, Compounds with π(loc) → π*(deloc) electronic transitions and their solvatochromism, J. Phys. Org. Chem. 28 (2015) 497–503.
[38] C.S. Dhanya, W.P. Sunita, P. Victor, R. Joseph, On improving the physiological stability of curcuminoids: Curcumininoid-silver nanoparticle complex as a better and efficient therapeutic agent, Nano-Structures Nano-Objects 25 (2021) 100661.
[39] M. Ghosh, S. Kundu, A. Pyne, N. Sarkar, Unveiling the behavior of curcumin in biocompatible microemulsion and its differential interaction with gold and silver nanoparticles, J. Phys. Chem. C 124 (6) (2020) 3905–3914.